Available online at www.sciencedirect.com
SCIENCE DIRECT®
ELSEVIER
Thin-Walled Structures 43 (2005) 209–224
THIN-WALLED STRUCTURES
www.elsevier.com/locate/tws

Buckling of cracked thin-plates under tension or compression

Roberto Brighenti*

Department of Civil Engineering, Environment and Architecture, University of Parma, Parco Area delle Scienze 181/A, 43100 Parma, Italy

Received 18 December 2003; accepted 27 July 2004

Abstract

Plates are easily susceptible to buckling under compression, in particular when plate's thickness becomes sufficiently small with respect to others plate's sizes; such a mode of failure is often prevalent with respect to strength failure. The buckling phenomena under tension loading can also occur, especially in plates containing defects such as cracks or holes; when the buckling load is reached, complex wrinkling deflection patterns in compressed regions develops around such imperfections.

In the present paper, the buckling analysis of variously cracked rectangular elastic thin-plates under tension and compression is considered. A short explanation of the buckling phenomena in plates is recalled and several numerical analyses, carried out by using the Finite Element Method (FEM), are performed in order to determine the critical load multiplier, both in compression and in tension, by varying some plates' parameters. In particular, the critical load multiplier is determined for different relative crack length, crack orientation and Poisson's coefficient of the plate's material which is made to range between 0.1 and 0.49.

Moreover a simple approximate theoretical model to explain and predict the buckling phenomena in cracked plates under tension is proposed and some comparisons are made with FE numerical results in order to assess its reliability in predicting buckling load multipliers.

Finally, the obtained results are graphically summarised (in dimensionless form) in several graphs and some interesting conclusions are drawn.

Keywords: Buckling; Wrinkling; Cracked tensioned plates; Fracture mechanics

* Tel.: +39 521 905 910; fax: +39 521 905 924.
E-mail address: brigh@unipr.it.

0263-8231/$ - see front matter © 2004 Elsevier Ltd. All rights reserved.
doi:10.1016/j.tws.2004.07.006

Nomenclature

a	crack half length
$a^* = a/W$	dimensionless crack length
A_n, B_n, C_n, D_n	coefficients involved in the solution of a deep beam under bending
$\mathbf{C}$	resultant of the compressive stresses along the X-axis in the interval $0 \leq x \leq b$
D	plate's flexural rigidity
E	plate's Young modulus
k	minimum value attained by a function of the dimensionless parameter $W^* = W/L$
K_{eq}	equivalent stress-intensity factor in Mixed mode of fracture
K_{I}, K_{II}	mode I and mode II stress-intensity Factors
K_{I}^*, K_{II}^*	dimensionless mode I and mode II stress-intensity Factors
K_{IC}	fracture toughness
L, W	plate's half length and width
N_x, N_y, N_{xy}	membrane and shearing forces (per unit length of the plate) in the corresponding directions
$\mathbf{R}$	resultant of the applied external uniform stress distribution σ_0
s	span of a deep beam corresponding to half of the cracked plate
t	plate's thickness
$t^* = t/W$	dimensionless plate's thickness
u_γ, u_η	displacements normal and parallel to the crack, respectively
$V(w(x,y))$	total potential energy
$\tilde{V} = V(\tilde{w}(x,y))$	approximate total potential energy
$w(x,y)$	plate's elastic surface (transversal displacements)
$\tilde{w}(x,y)$	transversal trial displacements plate's field
$W^* = W/L$	dimensionless plate's width
$\Phi(\xi,y)$	stress function
λ^-, λ^+	buckling stress multipliers in compression and in tension, respectively
ν	Poisson's ratio
θ	crack orientation angle
σ_0^-, σ_0^+	actual applied compressive or tensile stress, respectively
$\sigma_{\mathrm{E,c}}$	Euler buckling (uniform) stress in compression

1. Introduction

It is a common practical observation that plates can easily undergo to buckling collapse under membrane loading; this mode of failure can prevail over strength mode of failure, especially when plate's thickness is sufficiently small with respect to others plate's sizes. Even for plates under tension loading, the buckling phenomena can take place: it becomes a quite important occurrence particularly in structures where the presence of cracks or holes is involved. In these situations, tensioned plates can easily buckle, showing complex wrinkling deflection patterns in compressed regions around such defects.

The use of thin-walled high-strength panels in many technical fields—such as aerospace, mechanical, power industries, civil engineering applications and so on—is nowadays quite common. Since modern design process requires the evaluation of appropriate safety levels, many researches has been carried out in the last decades in order to quantitatively describe the buckling mode of failure in compression [1–3] or in tension [4–12] for such structures.

Few studies have been carried out to evaluate the influence of cracks on the buckling load in compressed or tensioned plates [13,14].

In the present paper, Finite Element (FE) analyses are performed to determine the critical load multiplier—both in compression and in tension—of variously cracked rectangular elastic thin plates; in particular, the effects of the cracks' length and orientation and the Poisson's coefficient of the plate's material (which is made to range between 0.1 and 0.49) are considered.

Moreover, a simplified and approximate theoretical approach is proposed to estimate tensile critical buckling stress for cracked panels containing cracks normal to the loading direction.

The obtained numerical and analytical results are graphically summarised (in dimensionless form) and compared and some interesting conclusions are drawn.

2. Formulation of the problem

The elastic surface $w(x,y)$ describing the plate's deflection when membrane loading are taken into account (Fig. 1a), can be obtained by solving the following well-known fourth-order partial differential equation (Von Kármán Love plate's theory) [15]

$$\nabla^4 w(x,y) = \frac{1}{D}\left(N_x w_{,xx}(x,y) + 2N_{xy} w_{,xy}(x,y) + N_y w_{,yy}(x,y)\right) \tag{1}$$

with appropriate boundary conditions; the notations $(\cdot)_{,ij}$ denotes the partial derivatives with respect to the geometric variables $i=x, y$, $j=x, y$, the operator ∇^4 is defined as

$$\nabla^4 \cdot = (\cdot)_{,xxxx} + 2(\cdot)_{,xxyy} + (\cdot)_{,yyyy} = \frac{\partial \cdot}{\partial x^4} + 2\frac{\partial \cdot}{\partial x^2 y^2} + \frac{\partial \cdot}{\partial y^4},$$

N_x, N_y, N_{xy} are membrane and shearing forces (per unit length of the plate's edges) in the corresponding directions, while $D = Et^3/12(1-\nu^2)$ is the usual plate's flexural rigidity

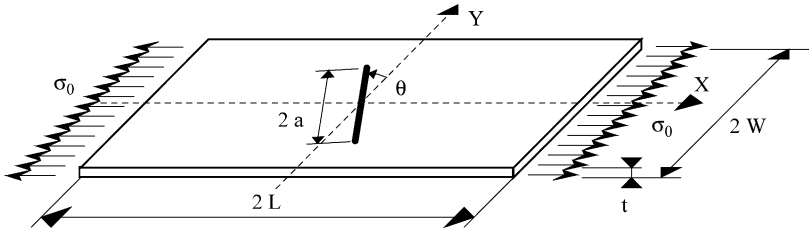

Fig. 1. Rectangular cracked thin-plate under uniform stress.

(E and ν are the Young modulus and Poisson's ratio of the material and t is the plate's thickness).

The closed-form solution of Eq. (1) can be obtained in a limited number of cases, usually characterised by simple geometry and boundary conditions.

For example, the case of a simply supported compressed uncracked rectangular plate (which are the boundary conditions in the present study) can be solved and the buckling stress $\sigma_{E,c}$ (Euler stress in a compressed plate) assumes the expression [15]:

$$\sigma_{E,c} = \frac{k\pi^2 D}{4W^2 t} \tag{2}$$

where k is the minimum value attained by a function of the dimensionless parameter $W^* = W/L$. Other expressions can be found for different boundary or loading conditions [15].

The buckling stress multipliers λ^- and λ^+ in compression and in tension, respectively, can be defined as the ratio between the actual applied stress, σ_0^- or σ_0^+, acting on the plate's edge and the buckling stress $\sigma_{E,c}$ of the compressed uncracked case (Eq. (2)):

$$\lambda^- = \frac{\sigma_0^-}{\sigma_{E,c}}, \quad \lambda^+ = \frac{\sigma_0^+}{\sigma_{E,c}} \tag{3}$$

For a given cracked plate's geometry, the buckling stress multiplier in compression λ^- is usually lower than the corresponding tension one λ^+; in an uncracked plate such difference becomes more and more pronounced and, sometimes, buckling in tension can be considered an unrealistic phenomena which often cannot practically occur. On the other hand, cracked plates can easily undergo to the buckling phenomena, even for relatively low values of the applied tension load (compared with compression buckling load), due to the compression zone that originates around the flawed area: the buckling mode in tension usually correspond to a local mode with complex membrane wrinkling deformed patterns.

3. Buckling of cracked plates under tension and compression

The buckling mode of failure of thin-walled structures, such as shells and plates, is a well-known phenomena and must be carefully considered in the assessment of structural safety because of its easy occurrence. In cracked members, such a phenomena can be even more crucial and special attention must be paid to such a structural failure mode.

As stated before, in thin plates subjected to tension, zones of compressive stress may develop close to existing cracks or geometry defects; as a consequence, structural local buckling phenomena may occur and the useful service life of the structured member can be heavily reduced leading to final fracture.

Such a local instability is responsible to out of plane displacements that take place in a limited portion of the panel, caused by loss of stiffness due to the effects of geometric non-linearity; in these problems the displacements must be considered and taken into account, since they have no negligible effects (as usually happens in linear problems) on the equilibrium configuration of the structural system.

3.1. Numerical FE evaluation of the buckling stress

In the present paper, a numerical investigation has been first carried out in order to evaluate the buckling stress multiplier of variously cracked tensioned and compressed plates.

The considered cracked plates have all their edges simply supported and are characterised by the following geometric parameters: main plate's length equal to $2L$, plate's width $2W$ and thickness t. A trough-the-thickness crack is assumed to exist in the centre of the plate, characterised by length $2a$ and orientation θ (measured counter-clockwise with respect to the direction orthogonal to the loading direction, Fig. 1). In order to define different cracked plates' configurations, some ratio between the above geometrical parameters have been assumed to be constant while others have been made to vary.

In particular, the following dimensionless geometrical parameters have been defined: plate's aspect ratio $W^* = W/L = 1/2$ (at which corresponds $k = 4$ in Eq. (2), [15]), relative plate's thickness $t^* = t/W = 1/200$, relative crack length $a^* = a/W = 0.1$, 0.2, 0.3, 0.4, 0.5 and orientation $\theta = 0$, 15, 30, 45, 60, 75, 90°.

The considered plates' material is supposed to be linear elastic and isotropic with Young modulus $E = 70{,}000$ MPa while different values of the Poisson's ratio ν have been assumed; in particular, the following values $\nu = 0.1$, 0.3 and 0.49 have been considered, the last one corresponding to a nearly incompressible material. The adopted finite element mesh is displayed in Fig. 2 where the element's refinement around the crack's tips and the use of quarter-point singular elements has been carefully considered (see detail A in Fig. 2) for an accurate evaluation of fracture mechanics' parameters.

In Fig. 3, the first and second buckling mode shapes for a cracked plate (characterised by $a^* = 0.5$, $\theta = 0°$ and $\nu = 0.3$) under compression (Fig. 3a and b) and under tension (Fig. 3c and d) are displayed. It is evident that the buckling mode shapes in compression correspond to a global phenomena with large and diffused out-of-plane displacements while the buckling phenomena in tension is much more localised around the cracked area.

In Fig. 4, the buckling load multipliers λ^- and λ^+, obtained by the FE analyses, are displayed against the relative crack length a^* for different crack orientation θ and Poisson's ratio ν. It can be noticed that the influence of Poisson coefficient becomes significant only for nearly incompressible cracked plates having cracks approximately

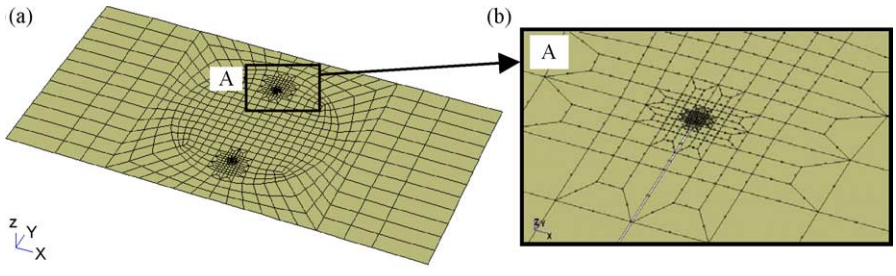

Fig. 2. Finite element mesh used for plate's buckling analyses (a); crack tip mesh detail (b).

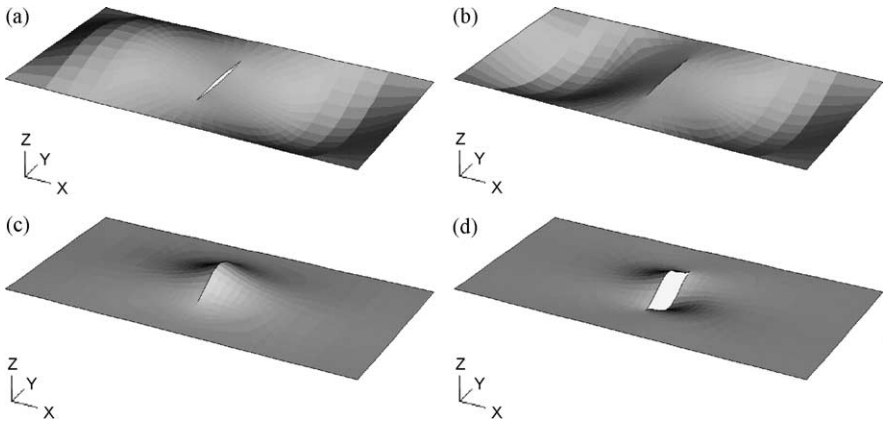

Fig. 3. First (a), second (b) buckling mode deflection shapes in compression and first (c), second (d) buckling mode deflection shapes in tension ($W^*=0.5$, $a^*=0.5$, $\theta=0°$).

parallel to the loading direction: in such cases the buckling stress is lower with respect to uncracked cases.

In tensioned cracked plates, it is also important to evaluate classical fracture mechanics parameters—such as the mode I (K_I) and mode II (K_{II}) Stress-Intensity Factors (SIFs)—to assess if the failure mode could be unstable fracture mode instead of buckling mode: in such cases, the fracture failure mode occurs when the critical SIF, K_{IC} (fracture toughness), is attained at the crack tip, i.e. $K_{eq}=K_{IC}$, where K_{eq} is an equivalent stress-intensity factor (to be used in mixed mode of fracture) obtained by taking into account simultaneously mode I and mode II SIFs [16].

In the case of an infinite plate under remote tension stress σ_0, with a crack of length $2a$ inclined of an angle $(\pi/2-\theta)$ with respect to the loading direction, the mode I (K_I) and mode II (K_{II}) SIFs are given by [17]:

$$K_I = \sigma_0 \cos^2\theta\sqrt{\pi a}, \quad K_{II} = \sigma_0 \sin\theta \cos\theta\sqrt{\pi a} \tag{4}$$

In the present study, the mode I and mode II SIFs have been evaluated by using the displacements correlation technique [18] applied to quarter point finite elements nodal results. By writing the displacement fields for a cracked plate under mode I or mode II loading [16]:

$$\begin{Bmatrix} u_\gamma \\ u_\eta \end{Bmatrix} = \frac{K_I}{2E}\sqrt{\frac{r}{2\pi}} \begin{Bmatrix} (1+\nu)\left[(2\kappa-1)\cos\frac{\alpha}{2} - \cos\frac{3\alpha}{2}\right] \\ (1+\nu)\left[(2\kappa+1)\sin\frac{\alpha}{2} - \sin\frac{3\alpha}{2}\right] \end{Bmatrix},$$

$$\begin{Bmatrix} u_\gamma \\ u_\eta \end{Bmatrix} = \frac{K_{II}}{2E}\sqrt{\frac{r}{2\pi}} \begin{Bmatrix} (1+\nu)\left[(2\kappa+3)\sin\frac{\alpha}{2} + \sin\frac{3\alpha}{2}\right] \\ -(1+\nu)\left[(2\kappa-3)\cos\frac{\alpha}{2} - \cos\frac{3\alpha}{2}\right] \end{Bmatrix} \tag{5}$$

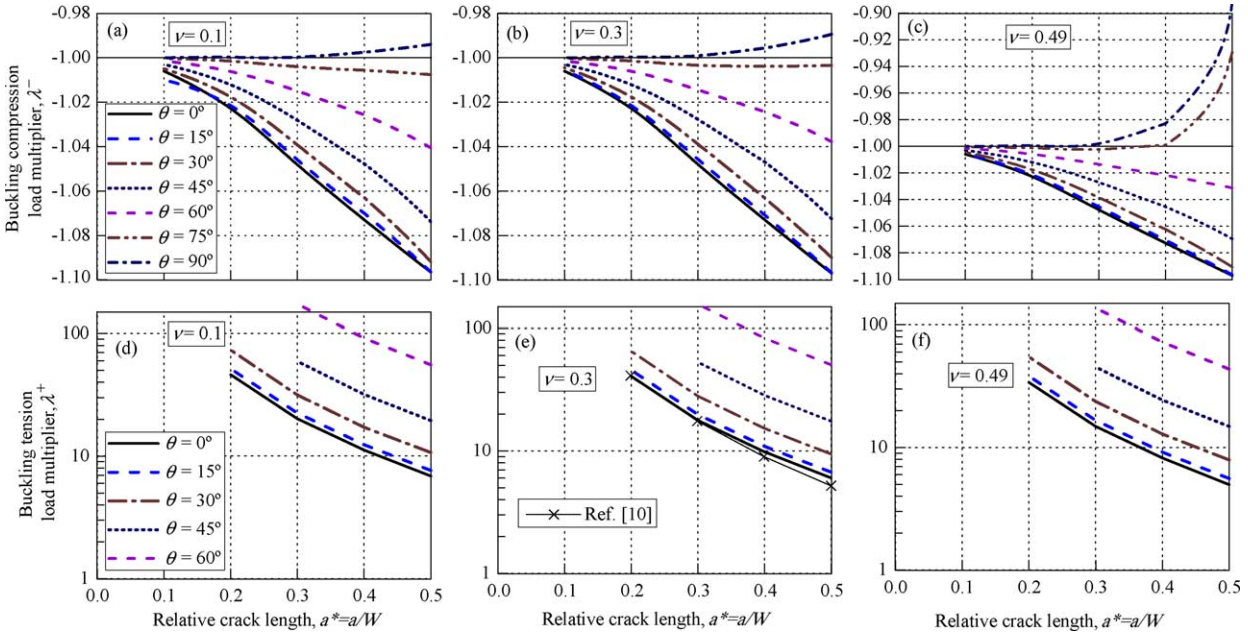

Fig. 4. Plate with all supported edges: buckling stress multipliers against the relative crack depth for various crack orientation θ, in compression ($\nu=0.1$ (a), $\nu=0.3$ (b), $\nu=0.49$ (c)) and in tension ($\nu=0.1$ (d), $\nu=0.3$ (e), $\nu=0.49$ (f)). Results by Riks et al. [10] are also displayed.

the corresponding SIFs can be evaluated. In Eq. (5) u_γ and u_η are the nodal displacements normal and parallel to the crack, respectively, α is the position angle of the considered point with respect to the crack direction, r is the distance from the crack tip, while $\kappa = (3-\nu)/(1+\nu)$ or $\kappa = (3-4\nu)$ in plane stress or plain strain conditions, respectively. In order to achieve a good accuracy, in the present study the mean value of the displacements measured at points near the crack tip (i.e. for $r \to 0$) belonging to the two opposite crack faces ($\alpha = \pm\pi$), are considered [18].

In Fig. 5, the mode I and mode II dimensionless SIFs, $K_{\mathrm{I}}^* = K_{\mathrm{I}}/(\sigma_0\sqrt{\pi a})$ and $K_{\mathrm{II}}^* = K_{\mathrm{II}}/(\sigma_0\sqrt{\pi a})$, are reported against the relative crack length a^* for different crack orientation θ and Poisson's ratio ν. It can be noticed that the present problem is a mixed mode fracture mechanics one, with the two extreme cases corresponding to pure mode I ($\theta = 0°$) and pure mode II ($\theta = 90°$). From the observation of Fig. 5, it can be noted that the mode I dimensionless SIF increases with the relative crack length and such a behaviour is more evident for high value of the orientation angle θ; for small cracks the mode I SIF tends to the theoretical value of an infinite cracked plate [17] (dashed lines, Fig. 5a–c). The Poisson's ratio value has a very limited influence on the mode I SIF.

Under mode II condition, the effect of the relative crack length is practically absent and the numerical K_{II}^* values are approximately equal to the theoretical ones [17] (dashed lines, Fig. 5d–f). As in the previous case, the Poisson's ratio has a very limited influence on the mode II SIF, too.

The knowledge of the SIFs allows a complete description of the stress field near the crack tip [16] and such a parameter is used in the following section to accurately identify the stress distribution in the plate's ligament.

3.2. Approximate analytical model for cracked plates in tension

Since buckling in cracked plates under tension is a localised phenomena, the critical load factor can be calculated, in an approximate way, by making simple considerations on an embedded compressed portion of the given tensioned plate.

From the observation of Fig. 4d–f, it can be deduced that the lowest tension buckling multiplier always corresponds to the case $\theta = 0°$; this is the more dangerous crack orientation under tension and it is thus considered in the following.

Due to the double axis of symmetry of the system (X- and Y-axes), only a quarter of the tensioned plate can be considered (Fig. 6). The qualitative stress distributions acting on the edges of such a portion of the plate are displayed in Fig. 6a: the external applied stress σ_0 (acting along the edge $x = L$), the stress $\sigma_x(y)$ (acting along the ligament, identified by $x = 0$, $a \le y \le W$, lying on the plate's Y-axis of symmetry) and the stress $\sigma_y(x)$ (acting along the edge $y = 0$, lying on the plate's X-axis of symmetry) are indicated together with the stress-free edges corresponding to the upper edge ($y = W$) and the crack face ($x = 0$, $0 \le y \le a$) of the plate.

The compressive stress acting along the plate's X-axis of symmetry in the interval $0 \le x \le b$, is responsible for the local buckling phenomena which occur when the external tension loading reach the critical value: $\sigma_{\mathrm{crit}}^+ = \lambda^+\sigma_0$.

The resultants of the above stress distributions are displayed in Fig. 6b; in particular, we can notice the resultant $\mathbf{R}$ of the applied external uniform stress distribution σ_0, which

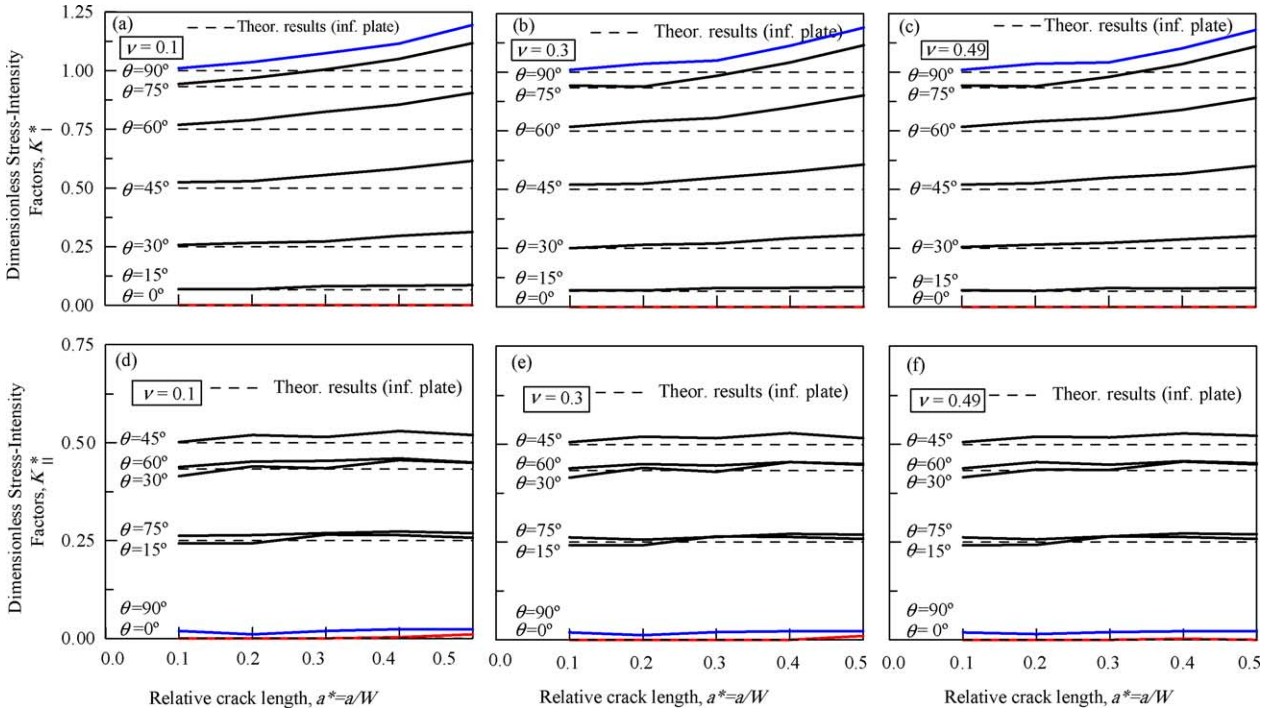

Fig. 5. Dimensionless SIFs against the relative crack depth a^* for various crack orientation θ: mode I ($\nu=0.1$ (a), $\nu=0.3$ (b), $\nu=0.49$ (c)) and mode II ($\nu=0.1$ (d), $\nu=0.3$ (e), $\nu=0.49$ (f)).

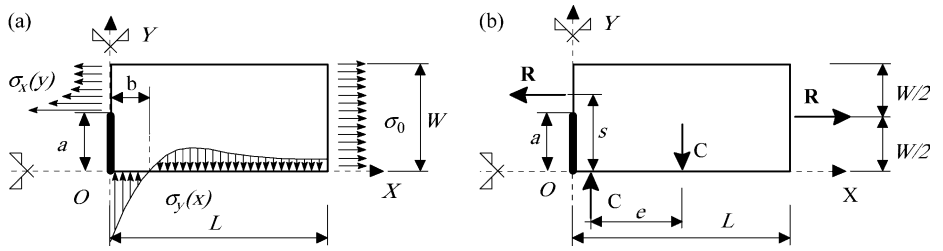

Fig. 6. Stresses σ_0, $\sigma_x(y)$, $\sigma_y(x)$ and resultants of the forces acting on the uniformly tensioned plate's axes of symmetry loading.

must be equal to the resultant of the stresses $\sigma_x(y)$ acting on the upper ligament of the cracked plate in order to satisfy the equilibrium condition in the X-direction. Such a resultant can be calculated as

$$\mathbf{R} = \sigma_0 W t = \int_a^W \sigma_x(x=0,y)t\,\mathrm{d}y \cong \int_a^{W_c} \left(\frac{K_I}{\sqrt{2\pi(y-a)}}\right) t\,\mathrm{d}y + (W - W_c)\sigma_0 t \tag{6}$$

where the near-tip stress field has been introduced, while W_c is the extension, measured from the crack tip, of the K_I-dominated stress field [16].

The position of the force $\mathbf{R}$, identified by the distance s from the X-axis, can be easily calculated by the previous stress distribution σ_x ($x=0$,y):

$$\begin{aligned} s &= a + \frac{1}{\mathbf{R}} \int_a^W \sigma_x(x=0,y)(y-a)t\,\mathrm{d}y \\ &\cong a + \frac{1}{\mathbf{R}} \left[\int_a^{W_c} \left(\frac{K_I(y-a)}{\sqrt{2\pi(y-a)}}\right) t\,\mathrm{d}y + (W - W_c)\sigma_0 \left(\frac{W + W_c}{2} - a\right) t \right] \end{aligned} \tag{7}$$

The resultant $\mathbf{C}$ of the compressive stresses (tensile stresses) acting on the X-axis in the interval under compression, $0 \le x \le b$ (under tension, $b \le x \le L$) is:

$$\mathbf{C} = \int_0^b \sigma_y(x, y=0)t\,\mathrm{d}y = -\int_b^L \sigma_y(x, y=0)t\,\mathrm{d}y \tag{8}$$

Such a compressive force can be considered to be responsible of the local buckling phenomena of a portion of the plate embedded in the main plate under study (Figs. 6a,b and 7b).

Such a compressed inner plate is characterised by complicated boundary conditions since it has completely free edges (the upper edge and the crack face) and variously tensioned or compressed loaded edges (Fig. 6a).

In order to theoretically solve the buckling problem of such a complex loaded plate, the stress distribution along the X-axis of symmetry of the considered structure is required.

By considering the portion of the plate lying in the half-plane $x > 0$ as a deep beam having height L and span equal to $2s$, supported by two finite width columns having approximately width equal to $c_w \cong 2(s-a)$, the stress field can be approximately evaluated by the use of the Fourier series expansion of the stress function $\Phi(\xi,y)$ [19] (a new

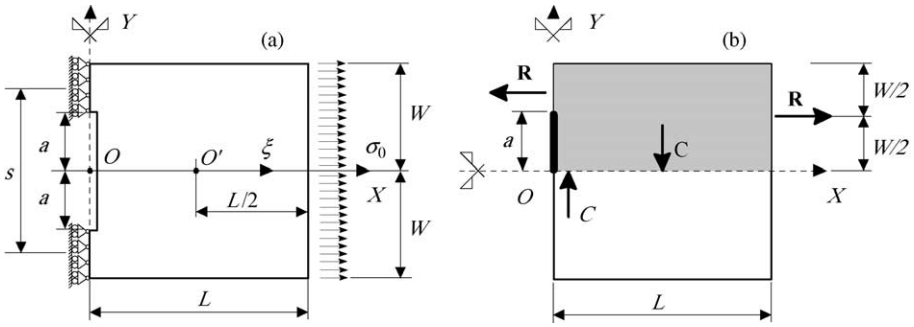

Fig. 7. Cracked plate considered as a deep beam (a). Scheme of the forces acting on 1/4 of the tensioned cracked plate; the compressive force C close to the crack is responsible of the plate's local buckling (b) of a plate under tension which undergo to local buckling due to transversal compression (filled area).

reference system (ξ,y), having origin in O' (Fig. 7), has been introduced). Writing the stress function in the form

$$\Phi(\xi, y) = \sum_{n=0}^{\infty} \Phi_n(\xi)\cos\,\alpha_n y \tag{9}$$

where $\alpha_n = 2n\pi/s$, the well-known field's equation $\nabla^2\nabla^2\Phi(\xi,y) = 0$ (which governs the plane elastic equilibrium problem in absence of body forces) becomes an ordinary fourth-order differential equation which can be simply solved [19]. The stresses can be obtained by deriving the obtained stress function as follows: $\sigma_x = \Phi_{,yy}$, $\sigma_y = \Phi_{,\xi\xi}$, $\tau_{x,y} = -\Phi_{,\xi y}$.

Finally, the following expressions can be found:

$$\sigma_x(\xi, y) = 2A_0 - \sum_{n=1}^{\infty} \left[A_n \cosh\,\alpha_n\xi' + B_n\alpha_n\xi' \cosh\,\alpha_n\xi' + C_n \sinh\,\alpha_n\xi' + D_n\alpha_n x \sinh\,\alpha_n\xi'\right]\cos\,\alpha_n y \tag{10a}$$

$$\sigma_y(\xi, y) = \sum_{n=1}^{\infty}[(A_n + 2D_n)\cosh\,\alpha_n\xi + B_n\alpha_n\xi \cosh\,\alpha_n\xi + (2B_n + C_n)\sinh\,\alpha_n\xi + D_n\alpha_n\xi \cosh\,\alpha_n\xi]\cos\,\alpha_n y \tag{10b}$$

$$\tau_{xy}(\xi, y) = \sum_{n=1}^{\infty}[(A_n + D_n)\sinh\,\alpha_n\xi + B_n\alpha_n\xi \cosh\,\alpha_n\xi + (B_n + C_n)\cosh\,\alpha_n\xi + D_n\alpha_n\xi \cosh\,\alpha_n\xi]\sin\,\alpha_n y \tag{10c}$$

where $\xi = x - L/2$, $\xi' = L/2 - x$ and the coefficients A_n, B_n, C_n, D_n assume the expressions:

$$
\begin{aligned}
A_n &= -(a_n + \bar{a}_n)\frac{\sinh(\alpha_n L/2) + (\alpha_n L/2)\cosh(\alpha_n L/2)}{\sinh(\alpha_n L) + \alpha_n L},\\
B_n &= (a_n - \bar{a}_n)\frac{\cosh(\alpha_n L/2)}{\sinh(\alpha_n L) - \alpha_n L},\\
C_n &= -(a_n - \bar{a}_n)\frac{\cosh(\alpha_n L/2) + (\alpha_n L/2)\sinh(\alpha_n L/2)}{\sinh(\alpha_n L) + \alpha_n L},\\
D_n &= (a_n + \bar{a}_n)\frac{\sinh(\alpha_n L/2)}{\sinh(\alpha_n L) + \alpha_n L}
\end{aligned}
\tag{11}
$$

with

$$
a_n = 0, \quad \bar{a}_n = -\frac{2\sigma_0 ts}{\pi c}\,\frac{(-1)^n}{n}\sin\left(\frac{n\pi c_w}{s}\right), \quad n = 0, \ldots, \infty.
$$

In Fig. 8, the dimensionless stress $\sigma_y(x,y=0)/\sigma_0$, acting along the X-axis of symmetry, calculated by the FE method and by the analytical expressions (Eq. (10)), are displayed for different relative crack length a^*. As can be observed, the numerical stress field along the X-axis is well approximated by the analytical expressions for all the considered cracked configurations and the compressed zone does not heavily depend upon the span of the deep beam (i.e. upon the relative crack length a^*). It should be noted that the analytical results

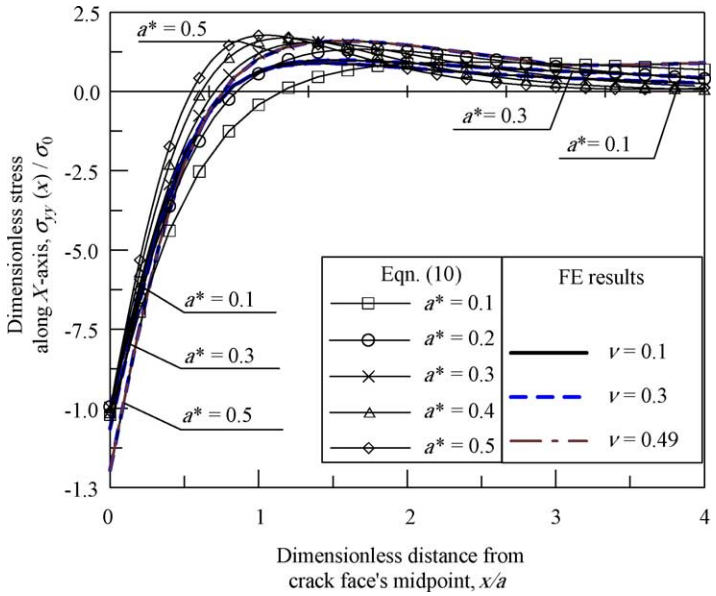

Fig. 8. Dimensionless FE stress distributions along X-axis in a cracked plate under tension in the case $\theta = 0°$ and $a^* = a/W = 0.1, 0.3, 0.5$. Results obtained by using Eq. (10) are reported (lines with symbols).

does not depend upon the Poisson's coefficient (see Eq. (10)); nevertheless also numerical results does not show appreciable dependence on such a material's parameter.

Once the stress distribution along the X-axis of symmetry of the plate is known, an estimation of the buckling load can be obtained since all the boundary conditions of the plate are now known.

The well-known Rayleigh–Ritz method [20] can be used to solve, in an approximate way, conservative mechanical problems by the minimisation of an adequate functional, such as the total potential energy $V(w(x, y))$. This approximate and simple approach is used in the present study.

The method works by writing a trial displacement field $\tilde{w}(x, y)$ as a linear combination of given functions (which satisfy a priori all the essential boundary conditions of the problem) multiplied by unknown parameters β_i, $i=1,\ldots m$; by writing the total potential energy $V(w(x, y))$ by using such an approximate displacement field, it becomes a function (not a functional any more) of the unknown parameters β_i which can be calculated by imposing the m stationariness conditions: $\tilde{V}_{,\beta_i} = V_{,\beta_i}(\tilde{w}(x, y)) = 0$.

By observing the first buckling mode shape pattern of a cracked plate under tension (Fig. 3c), it can be convenient to assume a one-parameter Gauss-like deflection shape function $\tilde{w}(x, y)$ to approximate the actual transversal displacement field

$$\tilde{w}(x, y) = \beta\, \mathrm{e}^{(\mathrm{LnC})\cdot[(x^2+y^2)/d^2]} \quad \text{or} \quad \tilde{w}(\rho) = \beta\, \mathrm{e}^{\ln c(\rho^2/d^2)}, \quad \text{with } \rho = \sqrt{x^2 + y^2} \tag{12}$$

where β is an unknown parameter and d represents the distance at which the displacement field $\tilde{w}(x, y)$ has decreased c times with respect to the value assumed in the origin, i.e. $\tilde{w}(x, y : \rho = d) = c\tilde{w}(0, 0)$, with $0 < c \ll 1$ (Fig. 9a).

By assuming that all the stresses are linearly dependent upon a single magnification factor and by inserting Eq. (12) in the expression of the total potential energy V written taking into account membrane loading, calculated over a quarter of the tensioned plate (filled area in Fig. 7b), an approximate evaluation of the function $\tilde{V} = V(\tilde{w}(x, y))$

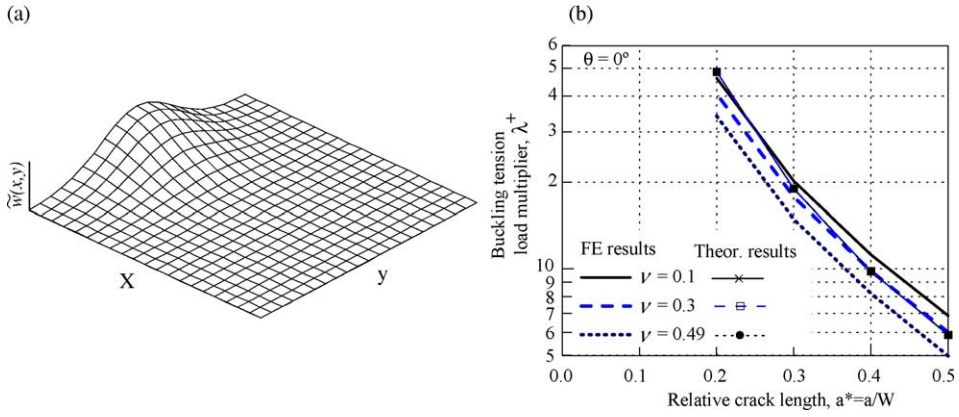

Fig. 9. Transversal displacement field pattern $\tilde{w}(x, y)$ used for analytical computation (a). Numerical and theoretical tension buckling stress multipliers λ^+ against the relative crack depth a^*, for $\nu = 0.1$, 0.3, 0.49 (b).

can be done:

$$\tilde{V} = \frac{D}{2}\int_0^W \int_0^L \left[(\tilde{w}_{,xx} + \tilde{w}_{,yy})^2 - 2(1-\nu)(\tilde{w}_{,xx}\,\tilde{w}_{,yy} - \tilde{w}_{,xy}^2) - \frac{N_y(x)\tilde{w}_{,y}^2 + 2N_{xy}(y)\tilde{w}_{,x}\,\tilde{w}_{,y} + N_x(y)\tilde{w}_{,x}^2}{D} \right] \mathrm{d}x\,\mathrm{d}y \tag{13}$$

The critical load multiplier λ^+ can be obtained by imposing the stationariness (which corresponds to the a minimum condition) of the approximate total potential energy $\tilde{V}$: this lead to a system of linear equations.

In Eq. (13), the membrane loading acting on the plate's edges are obtained as $N_x = \sigma_x(y)t$, $N_y = \sigma_y(x)t$ and $N_{xy} = 0$ (with positive values if they correspond to a tension loading) by using the stresses σ_x from the boundary conditions and σ_y obtained from Eq. (10b). The membrane loading considered in Eq. (13) are those acting along the edges $y = 0$, $x = L$ while the edges $x = 0$, $y = W$ have been assumed to be fixed and free of stress, respectively, so they have not been inserted in the approximate expression of the total potential energy $\tilde{V}(\tilde{w}(x, y))$.

The trial displacement field $\tilde{w}(x, y)$ (Eq. (12)) has been written by assuming $d = 2a$ and $c = 0.01$ (Fig. 9b).

In Fig. 9a, the critical load multipliers for a cracked plate in tension, obtained by the FE method and by the proposed procedure, are reported against the relative crack length for the three different Poisson's coefficients considered.

4. Discussion of the obtained results

The obtained numerical and theoretical results give important quantitative and qualitative information about the buckling behaviour of cracked damaged plates under tension and compression.

In Fig. 4, the buckling load multipliers λ^- and λ^+, obtained by the FE analyses, are displayed against the relative crack length a^* for different crack orientation θ and Poisson's ratio.

It can be noticed that for a given relative crack length a^*, the compressive load multiplier λ^- decrease (in absolute value) by increasing the orientation angle θ from 0 to 90°; in the case $a^* = 0.5$, for example, the difference between the two extreme cases considered ($\theta^\circ = 0$ and 90°), is approximately equal to 10% for $\nu = 0.1$ and 0.3 while it becomes equal to 20% for $\nu = 0.49$ (nearly incompressible material). Such a difference tends to vanish decreasing the relative crack length (Fig. 4a–c).

Decreasing the crack length, λ^- tends to assume the value of the uncracked case ($\lambda^-_{\text{uncracked}} = -1$). It is interesting to note that, in general, the presence of the crack seems to have a beneficial effect (regardless of the crack orientation) since it increase the compressive buckling stress with respect to the uncracked case. A slightly lower buckling load is produced by cracks parallel, or nearly parallel, to the loading direction (i.e. $\theta \cong 90^\circ$).

The tension critical load multipliers λ^+ (Fig. 4d–f) are much higher than the corresponding compressive ones and tend to increase rapidly by reducing the crack length and increasing the crack orientation angle from 0 to 90° (note that in Fig. 4d–f, the load multiplier axis is in logarithmic scale). The case of a crack perpendicular to the loading direction always corresponds to the lowest buckling load, so this crack orientation can be considered to be the most dangerous in tension. Results by Riks et al. [10] are also represented in Fig. 4e and the agreement with present results can be considered to be quite satisfactory.

The increase of the Poisson's coefficient has the effect to reduce the buckling load in tension, while the curves patterns are not significantly modified by changing this parameter.

Approximate theoretical results are reported in Fig. 9b for the case $\theta = 0°$ together with FE results. As can be observed, the numerical tension critical load multipliers λ^+ are approximated with an acceptable accuracy by theoretical results; the dependence upon the Poisson's coefficient is practically not reproduced by the proposed theoretical model while this dependence is evident from numerical results. Nevertheless theoretical results are always within the range defined by the two extreme cases, $\nu = 0.1$ and 0.49 and can be considered to give the buckling load multiplier with an acceptable accuracy. The proposed approximate theoretical procedure can be considered a simple and fast way to evaluate tensile buckling stress in cracked plates.

5. Conclusions

In the present paper, the buckling phenomena of variously cracked rectangular elastic thin-plates under tension and compression has been considered.

Numerical Finite Element Method (FEM) analyses have been performed in order to determine the critical load multiplier, both in compression and in tension, by varying some cracked plates' parameters. In particular, the effects of the relative crack length, crack orientation and Poisson ratio of the plate's material on the buckling phenomena have been investigated.

A simplified and approximate theoretical procedure has been proposed to evaluate the critical load of cracked tensioned plates by using the stress field of a deep beam (to which the cracked plate can be compared) and the Rayleigh–Ritz method applied to a portion of the given plate, with an adequate choice of the trial displacement field corresponding to a local buckled plate.

Numerical investigations have shown that the main crack's effect is the reduction of the buckling compressive stress multipliers λ^-, especially for low values of the orientation angle θ. The Poisson's ratio values have important effects only for nearly incompressible materials ($\nu = 0.49$) when the crack orientation angle θ is greater than approximately 60°. In general, the presence of a crack in a compressed plate has a beneficial effect (regardless of the crack orientation) since it increases the compressive buckling load with respect to the uncracked case. The tension critical load multipliers λ^+ have shown the tendency to be higher than the corresponding compressive ones; furthermore they tend to increase rapidly

by reducing the crack length and increasing the crack orientation angle. In cracked tensioned plates, the crack orientation $\theta = 0^\circ$ can be considered to be the most dangerous.

The results given by the simple approximate theoretical proposed model have been compared with numerical results and the accuracy achieved has been quite satisfactory. The proposed approximate theoretical procedure can be considered a very simple tool to assess tensile buckling stress in cracked plates, without the need of more complex FE analyses.

Acknowledgements

The author gratefully acknowledges the research support for this work provided by the Italian Ministry for University and Technological and Scientific Research (MIUR).

References

[1] Wang CM, Xiang Y, Kitipornchai SK, Liew M. Buckling solutions for Mindlin plates of various shapes. Eng Struct 1994;16:119–27.
[2] Matsunaga H. Buckling instabilities of thick elastic plates subjected to in-plane stresses. Comput Struct 1997;62:205–14.
[3] Jiang W, Bao G, Robert JC. Finite element modeling of stiffened and unstiffened orthotropic plates. Comput Struct 1997;63(1):105–17.
[4] Friedl N, Rammerstorfer FG, Fischer FD. Buckling of stretched strips. Comput Struct 2000;78:185–90.
[5] Markström K, Storåkers B. Buckling of cracked members under tension. Int J Solids Struct 1980;16:217–29.
[6] Sih GC, Lee YD. Tensile and compressive buckling of plates weakened by cracks. Theor Appl Fract Mech 1986;6:129–38.
[7] Shaw D, Huang YH. Buckling behavior of a central cracked thin plate under tension. Eng Fract Mech 1990; 6:1019–27.
[8] Shaw D, Huang YH. Buckling behavior of a central cracked thin plate under tension. Eng Fract Mech 1990; 35:1019–27.
[9] Shimizu S, Enomoto SYN. Buckling of plates with a hole under tension. Thin-Walled Struct 1991;12:35–49.
[10] Riks E, Rankin CC, Brogan FA. The buckling behavior of a central crack in a plate under tension. Eng Fract Mech 1992;43:529–47.
[11] Estekanchi HE, Vafai A. On the buckling of cylindrical shells with through cracks under axial loading. Thin-Walled Struct 1999;35:255–74.
[12] Guz AN, Dyshel MSh. Fracture and buckling of thin panels with edge crack in tension. Theor Appl Fract Mech 2001;36:57–60.
[13] Vafai A, Javidruzi M, Estekanchi HE. Parametric instability of edge cracked plates. Thin-Walled Struct 2002;40:29–44.
[14] Barut A, Madenci E, Britt VO, Starnes JR. Buckling of a thin, tension-loaded, composite plate with an inclined crack. Eng Fract Mech 1997;58:233–48.
[15] Timoshenko SP, Gere JM. Theory of elastic stability, 2nd ed. New York: McGraw-Hill; 1961.
[16] Broek D. Elementary engineering fracture mechanics. Dordrecht: Martinus Nijhoff Publishers; 1982.
[17] Irwin GR. Analysis of stresses and strains near the end of a crack transversing a plate. Trans ASME, Ser E, J Appl Mech 1957;24:361–4.
[18] Lim IL, Johnston IW, Choi SK. On stress intensity factor computation from the quarter-point element displacements. Commun Appl Numer Meth 1992;8:291–300.
[19] Flügge W, editor. Handbook of engineering mechanics. 1st ed.. New York: McGraw-Hill; 1962.
[20] Langhaar HL. Energy methods in applied mechanics. New York: Wiley; 1962.